FORMAL CHARACTERISTICS OF ALUMINIUM BURNING RATE LAW IN NON-IDEAL DETONATIONS OF AMMONIUM NITRATE BASED MIXTURES

Komissarov P. (1), Ermolaev B. S. (1), Khasainov B. A. (2), and Presles H.-N. (2)

(1) N. Semenov Institute of Chemical Physics Russian Academy of Sciences, MOSCOW, Russia
(2) Laboratoire de Combustion et de Détonique, UPR CNRS 9028, ENSMA, Poitiers, France

ABSTRACT

Detonation velocity of the ammonium nitrate (AN) + Al mixtures in loose-packed charges confined in 2-mm thick 1-m long steel tubes has been measured. Parameters varied were AN particle size (porous prills as supplied and two grinded unsieved fractions), Al particle size (spherical fine and coarse powders), Al content in the mixtures (from 0 to 18 wt. %) and tube diameter. Depending on the varied parameters, the detonation velocity ranges from 1200 up to 4000 m/s. Several runs were equipped with the PVDF-gauges to record pressure profiles. The experimental database has been used to extract aluminium burning rates. A simple model of steady non-ideal detonation developed in the quasi-1D approximation for weekly diverging flow in multiphase reactive medium was used for numerical analysis of the database. Values of coefficients specifying rates and pressure dependence of AN surface burning and diffusive Al burning in the AN decomposition products were fitted to provide the best agreement between numerical modeling and experiment

.

INTRODUCTION

Rate of aluminum burning in detonation products of condensed explosives is still a subject of intensive investigation and discussions. For deducing the corresponding information, the cylinder test is typically used, and experimental data are analyzed by gasdynamic codes (see, for example, [1]). However, the effect of Al burning manifests itself in pretty small changes of the velocity vs. expansion diagram, and results of analysis seem to be extremely sensitive to accuracy of experimental data and EOS of detonation products. Besides, due to absence of a generally accepted physical model of Al burning in detonation products, different authors use different formal laws to describe the Al burning rate which include dependencies on Al particle size, concentration of oxidizing species in HE, and, sometimes, on pressure.

In this work, in order to extract information on Al burning rate we used experimental data on the charge diameter effect on detonation of ammonium nitrate (AN) + Al mixtures confined in 2-mm thick 1-m long steel tubes. This approach has a few advantages. Measurements are simple, and the effect of Al burning manifests itself by the marked increase of detonation velocity. As a consequence, extensive database can be easily obtained and simply analyzed with no severe requirements being led to the theoretical model applied.

Parameters varied are AN particle size (porous prills as supplied and two grinded unsieved fractions), Al particle size (spherical fine and coarse powders), amount of Al in mixture (from 0 to 18 wt. %) and tube diameter. The detonation propagation was monitored using a set of 11 optic fibers positioned uniformly along the confinement. Depending on the varied parameters, the detonation velocity ranges from 1200 up to 4000 m/s. Several runs were equipped with the PVDF-gauges to record pressure profiles.

To deduce Al burning rates, a simple model of steady non-ideal detonation developed in the quasi-one-dimensional approximation for weekly diverging flow in multiphase reactive medium was used. Equations specifying rates of AN surface burning and diffusive Al burning in the AN decomposition products comprise 4 coefficients (the burning rate coefficient and the pressure exponent for both components). Values of these coefficients were fitted to provide the best agreement between numerical modeling and experiment.

TECHNIQUE OF EXPERIMENTS

Experiments have been performed with AN in prills as supplied (industrial ammonium nitrate produced by Grand Paroisse composed of porous spherical prills of 0.5 – 1.5 mm in size) and two fractions of grinded unsieved AN with average particle size 40 μm (fine) and 120 μm (coarse). AN prills were preliminary dried ensuring that humidity does not exceed 0.3 wt. %. The grinded fractions of AN were produced by using two operating modes of a mill different in duration. Maximum of the size distribution in polydisperse powders was near 40 and 250 μm (Fig. 1). Three different marks of spherical aluminum with particles 5, 45 and 100 μm in size were used. Components were mixed manually to avoid crushing the AN prills. Components in a preset amount were poured into a 1-litre glass bulb filling a half of its volume and vigorously shaken during 15 min. To avoid stratification, the mixtures with the 18.5% Al were subjected to additional mixing during 10 min by the use of a plastic stick 12 mm in diameter, making circular movements (about 600 – 700 cycles in total). The mixtures with 2, 8 and 18.5 wt. % Al of loose-packed density have been studied. The 1-m long steel tubes (trademark TN37B) 8, 12, 16, 21 and 31 mm in internal diameter and 2-mm wall thickness were used.

The mixture prepared was poured in portions into the vertically fixed, steel confinement with the bottom end closed by a thin Al foil. During the mixture loading we controlled the average density of the mixture column to ensure absence of voids. After the mixture filled the total tube length, the average charge density was determined, and then a 30 mm long layer of the mixture was deleted from the top end of the tube and replaced with a booster. Then the confinement (equipped and loaded) was transported, being kept in the vertical position, into the explosion chamber and fixed vertically with 50-mm spacing between the bottom tube end and the chamber floor.

The booster was made of the condensed plastic explosive (with detonation velocity of about 7000 m/s) near 50 mm in length; it occupies the 30-mm end piece of the confinement being in a close contact with the mixture and partially getting outside the tube end. The booster mass depends on charge diameter. The preliminary runs carried out with the 21-mm charge diameter have demonstrated that the 25-g booster provides reliable initiation of the AN + 18.5% Al (5 μm) mixture. Later we used the same booster with all other mixtures shooting in the 21-mm tubes. With the charges of other diameters we used the 12-g booster for 8-mm tubes, 15 g for 12-mm, 20 g for 16 mm and 50 g for the 31 mm, correspondingly. A standard detonator-cap No 8 was used to initiate the booster. Schematic of the setup is shown in Fig. 2.

Detonation velocity was recorded by using 11 light emission probes spaced with a regular 90-mm interval along the charge confinement. For this purpose each confinement had a raw of small orifices drilled in it; steel capillaries 0.75 mm in internal diameter were inserted into these orifices, being flush with the internal surface of the tube channel. Optical fibre was glued into the capillary leaving a 5-mm spacing between the fibre end and the internal surface of the tube channel. Hereby, the free end of the capillary served as the objective aperture reducing the volume from which the light emission approaches the fibre and enhancing the measurement accuracy. All 11 optical fibres were connected to a collector located directly near the confinement. To reduce the light emission losses in the collector, the receiving fibre which connects to the photo-detector was equipped with a polycarbonate lens. The lens is produced out of a cheap transparent light-emitting diode 5 mm in diameter with the light beam divergence angle equal 12.5^{o}. To ensure reliable recording, because in different AN + Al mixtures the light emission intensity may strongly differ, the signal of the photo-detector was monitored simultaneously by two channels of the oscilloscope with various sensitivity. In some runs only part of optical fibers was collected to one channel by the lens. Another fibers were connected to the scope separately.

Fig. 3 shows an example of recording the detonation front propagation along a charge, obtained using a set of optic fiber probes. In this run, 7 first probes were connected to the collector and their signals were recorded by the first channel whereas each signal of the last probes was recorded by the separate channels. As is seen, signals recorded separately have markedly higher amplitude than those recorded through the collector; however, the signal width also increases. To determine the time instant when the front passes by the probe a point of the maximum rise rate of the signal was conditionally used. Starting from the first probe up to the last one, the time interval between actuation of the adjacent probes increases and then levels at a nearly constant value. This corresponds to decrease of the initial velocity of the wave propagation caused by a power detonation impulse of the booster, and a successive build-up of the steady detonation mode. Although the “instrumental” inaccuracy of the wave velocity does not exceed 20 m/s, acquisition of experimental data shows that there are fluctuations of the wave velocity along the charge length with markedly higher amplitudes. The possible reason of these fluctuations is an irregularity of the charge density along the tube which turns out unavoidable, especially for the Al-rich mixtures loading into tubes of a rather small diameter.

MEASUREMENTS OF DETONATION VELOCITY

Here to characterize the detonation velocity we use a value averaging the wave propagation velocities for three last bases of measurements.

Fig. 4 shows the average detonation velocity versus internal diameter of the confinement for mixtures of AN in prills with three different fractions of spherical aluminum particles. All runs for the AN + 18.5 % Al (5 μm) mixtures demonstrate transition to a steady detonation. As the charge diameter decreases from 31 up to 8 mm, the detonation velocity monotonously decreases from 3000 to 1550 m/s. Detonation velocities recorded in the charges with 8 % Al (5 μm) of the same diameters are almost identical to the previous ones. Mixture with 2 % Al also shows establishing a steady detonation mode in all charge diameters tested. However, in contrary to the previous mixtures when the detonation velocity drops monotonously with decreasing the charge diameter, in this series the charges 12, 16 and 21 mm in diameter demonstrate almost identical detonation velocity (1630 – 1720 m/s). And only in the 31-mm charge the markedly higher detonation velocity was observed (2230 m/s).

For the mixtures with mean Al particles (45 μm) the transition to steady detonation proceeds slower and often takes more than a half of the charge length. The 31-mm and 21-mm diameter charges with 18.5 % Al mixture demonstrate a steady detonation at 2550 and 2250 m/s, respectively. In the 16-mm charge the wave propagates with permanently descending velocity up to two last bases of measurement near the charge end where it levels at 1500 m/s. In the 12-mm charge the detonation fails. Thus the critical diameter of a detonation for this mixture is about 16 mm. In all runs with 8 % Al mixture of this series the wave propagation velocity reduces while the wave approach the charge end, and one can assume that the 1-m charge length is short for establishing a steady detonation mode. In the 12 mm charge which (taking into account the sizes of the confinement fragments) seems to be close to the critical detonation diameter, the wave propagates with strong fluctuations of the velocity; the reason, more likely, is due to non-uniformity of charge density along the tube.

Almost all runs conducted with coarse Al particles (100 μm) demonstrate wave propagation with a smoothly decreasing velocity along the total charge length. Nevertheless, the detonation velocity does not differ markedly in comparison with the AN + Al (45 μm) mixtures at the same charge diameter and Al content. For the mixtures with 18.5 % Al (100 μm) only charges 16, 12 and 8 mm in diameter were fired. Strong fluctuations of the wave velocity in 8-mm diameter are caused by non-uniformity both of the charge density and Al particle concentration along the charge. Only in the 16-mm charge filled with 8% Al (100 μm) the wave velocity is stabilized near the charge end; in the charges 31, 21 and 12 mm in diameter the evident decrease of the wave velocity at the last bases of measurement is observed. The final detonation velocity only slightly depends on the charge diameter and ranges between 1200 and 1400 m/s.

Mixtures with grinded AN were studied using predominantly the fine 40-μm fraction of AN. Three sets of experiments was carried out. Each set was conducted with different fractions of Al particles. In total, detonation velocities are higher than in the case of AN in prills and increase as the charge diameter increases.

First set was conducted with 5-μm Al powder. Experiments was comducted in 8, 12, 16 and 21 mm tubes. Poor mixtures with 2 wt.% demonstrates continuous behavior without velocity perturbation along the tube. The detonation velocity increases with diameters and varyed from 2600 m/s for 8mm carge to 3150 m/s for 21 mm charge respectively. Velocities are higher then in case of AN in prills. Fragments from 8 mm tube shows that critical diameter is close. In experiments with 8 wt.% of metal fuel the velocities also increased with diameters (3350-4030 m/s), however at the end of the tube velocities demonstrates a tendency to be higher then in the middle. The confinement fragments for all shots have a pretty little size (about 4-6 mm). In case of 18.5 wt.% Al the detonation velocities are lower than in the case of 8% mixture (3000-3650 m/s).

For the next set of runs with the mean 45-μm Al particles velocities are lover then in case of 5-μm Al mixtures of same richness. This set conducted with 8-31 mm tubes. A critical diameter detected in 12 mm tube filled with poor 2 wt.% mixture – in this case detonation stops after 25 cm. Detonation velocities level for 2% mixture 2150-3100 m/s for 12-21 mm tubes respectively. In comparison with previous set of experiments in this set conducted with 8 wt.% of 45 μm Al, velocities decreases its level (2850-3900 m/s) and demonstrates some perturbations at the beginning in tubes of 16-31 mm. In all runs the velosity have a tendency to rise after first half of the tube. Charge in 31 mm diameter shows lower velocity then 21 mm. Experiments with 18.5 wt.% mixtores of same Al fraction shows quite big velocities perturbations at the beginning of the tube. Rich (18.5%) mixtures demonstrates aloso higher velocities interval then in previous set (3350-3930 m/s). Note the lower velocity for 31 mm tube then for 21 mm as in case of 8% mixture.

Last set of experiments was comducted with the coarse 100-μm Al particles. In all runs with poor (2 wt.%) mixture detonation stops after first 20-40 cm. For 8 wt.% mixture critical point was at 8 mm and velocity level for 12-21 mm tubes was 2850-3500 m/s. It slightly lower then in case of 45-μm Al particles of the same richness. At internal diameters 16 and 21 mm velocities have a tendency to rise and have near same levels as in case of 45 mixtures of same richness. Summarized results of this experiments also presented in figure 4.

For 3 sec fractions of AN only selected experiments was performed just to show difference relatively 30 sec mixtures. Sowed at fig. 4 results also demonstrates influence of AN particle size on detonation velocity for 8 and 12 mm in ID tubes filled with 8% mixtures. Clearly seen that decreasing of AN particles sizes drastically increases detonation velocity. Comparison of results for 2% and 18.5% mixtures in 8 and 12 mm tubes with different AN particle sizes demonstrates that AN particle sizes influent on detonation velocity in all cases and increased they when AN size decreased.

PRESSURE MEASUREMENTS

In the selected runs tube casing was equipped with home-made PVDF gauges. We relied upon a gauge design described in [Borisenok, et al (2003), Soulard, et al (1990)]. As a sensitive element of the gauge we used the metallized, bi-oriented PVDF film of 25 μm thick manufacturing by Piezotech S.A. Co. The sensitive element is a square of 9 mm^2. To get off the electrical charge generated by the sensitive element, 5-μm Al foils of 1.3 mm in width bonded to the 50-μm Cu foils of 3 x 10 mm in sizes were used. The assembly glued between two 50-μm PVC films. A final thickness of the PVDF gauge equals 127 ± 5 μm. As the surface area of sensitive elements can differ by ±3 % the sensitivity factor must be corrected to take into account this difference. The gauges were calibrated by using pendulum techniques as described in [ссылка на Якушева]. Signals of the accelerometer and the PVDF gauge generated by impact were recorded simultaneously. The pressure between the steel cylinders measured with a help of accelerometer was then compared to the gauge signal, and the gauge sensitivity factor was determined. During calibration and during detonation runs the gauge is connected to the oscilloscope through a passive integrating unit which is produced with a 50-Ohm electrical line, matching resistor and 220 nF capacitor. After several loadings during the calibration of the gauge its thickness can change. For this reason during the mechanical calibration we controlled the gauge thickness and rejected the gauge if its thickness decreased by more than 3 μm. Besides, during calibration we also controlled the gauge capacity. Average value of the gauge capacity after calibration equals 10 pF, and the total capacity of the measuring circuit equals 0.531 nF. Typical value of the sensitivity factor of the PVDF gauge embedded into the measuring circuit equals 0.48 volt/GPa. For the higher pressure range (above 1 GPa) PDVF gauges sensitivity were corrected by using polynomial approximation discussed in [Nabatov, etc. (1994), Molodets, etc. (1994)] according to which the sensitivity of PVDF gauges reduces with the pressure increase. In experiments PVDF gauge was mounted inside the tube trough the slit on the wall, usually in front of optical fiber to be sure about record position. The gauge was inserted inside the tube, so that PVDF sensor was located closer to the tube axis. No any glue was used to fix gauge on the tube. The side of the wall where gauge touch metal is quite important. It must be side of the slit opposite from

detonation wave direction. In another case the signal noise is increased drastically. Also important to ground the bottom end of the tube, else the noise will be also very strong and zero level of the signal moved in course of shoot due to difference in potentials between scope and reacting mixture.

Pressure measurements performed in case of the mixtures with non-grinded ammonium nitrate shows quite different patterns of the pressure traces. The possible reason is irregular contact between PVDF sensor and AN grains. In case of mixtures with grinded AN more reproductive signals were recorded. Seclected examples of pressure traces for experiments with 30 sec grinded AN for diffrernt tube diameters, richness of the mixture and Al particle sizes are represented in figure 5. In all selected runs after first spike clearly seen planar plateau. Duration of this plateau allow as to beleive in fidelity of the shape of the signals and approximate amplitude behind first spike. As regards the first spike, the signals accompanied with high-frequensy oscillations, apparently linked with multiple shock wave reflection inside the gauge.

MODEL

Theoretical analysis of experimental data on detonation velocity – charge diameter effect is traditionally applied to infer information on chemical conversion rates of solid explosives. AN+Al compositions are especially convenient for this purpose because of high sensitivity of their detonation properties to the charge diameter and confinement. It allows one, by fitting calculations to experimental data, to get rather exact estimations of the chemical conversion rate and its pressure dependence.

Here for numerical analysis of the available database we use a simple model of steady non-ideal detonation developed in the quasi-1D approximation for weekly diverging flow in multiphase reactive medium. Equations specifying rates of AN surface burning and diffusive Al burning in the AN decomposition products comprise 4 coefficients (the burning rate coefficient and the pressure exponent for both components). Values of these coefficients were fitted to provide the best agreement between numerical modeling and experiment.

The model considers the steady-state reaction zone in a self-sustaining detonation wave that propagates with a constant velocity D along the axis of a cylindrical charge of explosive material of radius r^*. Main items of the model are as follows.

(1) We use the classical quasi-1D approximation [Wood and Kirkwood ?] for a weekly diverging flow in multiphase reactive medium [Nigmatulin (1987)]. This approximation enables us to reduce the problem to a integrating a set of ODE with boundary conditions set at the shock front.

(2) The reactive medium is a mixture of the initial components and of the products of their final chemical conversion. For instance, in the case of an explosive composition made of AN and Al, the reactive mixture includes 4 species: (1) the solid AN, (2) the products of AN chemical conversion, (3) the solid Al and (4) the products of Al burning in the AN conversion products. The state of the reactive medium is determined by the mass fractions of these 4 species (η_i) with the mixture density and internal energy calculated from the species density (ρ_i) and internal energy (e_i) by using the additivity rule. We assume that all species are in local mechanical equilibrium (identical pressure P and material velocity U), and that species (2) and (4) have identical temperature which, however, differs from the temperatures of the solid species.

(3) The chemical reaction is assumed to proceed in the surface burning mode. That is the reason to use the aforesaid condition that there is no heat equilibrium between solid components and conversion products. In this case the conversion rate could be expressed as the product of the specific surface and of the burning rate. However, these two parameters are unknown, and in our model, the chemical conversion rate is described as the function of species contents and pressure, which includes a scaling factor applied as a fitting parameter. The intensity of the chemical conversion of the explosive material per unit volume is thus given by

$$M_1 = \rho_{10}(\eta_1/\eta_{10})^{2/3} G_1 (P/P_{ref})^n \qquad (1)$$

where ρ_{10} and η_{10} designate the theoretical maximal density (TMD) and the initial mass fraction of the species (1). The pressure parameter P_{ref} is introduced for convenience in order to express the burning coefficient G_1 in sec^{-1} irrespective of the pressure exponent n and is set to 1 GPa. Hence, only two parameters G_1 and n are varied to obtain the best agreement between numerical modelling and experiment.

(4) The relation used to calculate the intensity of Al burning is

$$M_3 = \rho_{30} G_3 (\eta_3 / \eta_{30})^{2/3} (P / P_{ref})^r (\frac{C_{ox}}{1 + \eta_4 / \eta_2})^s \quad (2)$$

Here C_{ox} designates the molar fraction of the active oxidizing gases in the species (2) that participate into Al oxidation. The multiplier comprising C_{ox} accounts for the dependence of the Al burning rate on concentration of these gases. In the case of the AN + Al mixtures we have set C_{ox} = 0.71 and s = 1.0. We have set the pressure exponent r = 0 because one can expect that there is no strong pressure influence on the Al burning rate at elevated pressures. Thus, only the coefficient G_3 of the Al burning rate is used as an adjustable parameter.

(5) The surface burning of AN follows the chemical reaction initiation at hot spots generated in the shock wave front. We treat the wave front as a common shock discontinuity. From a physical viewpoint it means that all the relaxation processes which take place during shock loading of a porous explosive material and result in mechanical equilibrium are much faster than the chemical conversion time. Both the chemical reactions in hot spots and filling of pores with reaction products which contribute into pressure relaxation at a meso–scale level are main components of the shock loading process of porous HE and should be attributed to the wave front. Finally, we assume relying upon arguments considered in [, Khasainov, et al (1996] that (i) the burning of AN described by Eq. (1) begins just behind the shock wave front with no ignition delay; (ii) the amount η_{2f} of AN consumed during the hot spot process is small and set equal constant 0.01; (iii) delay of Al burning is also ignored.

(6) Values of variables at the wave front (designated by index *"f"*) are determined by solution of a set of traditional algebraic Rankine-Hugoniot conservation equations through the shock discontinuity in the mixture. To close this equation set we assume following [Mader (1979)] that the shock compression energy shears between solid components in reverse proportion to their shock impedance.

The system of ordinary differential equations (ODE) in the reference frame attached to the wave front ($x \geq 0$):

Equations of conservation of mass, momentum and energy of the mixture

$$\frac{d}{dx}(\rho U) = -\rho U \frac{d}{dx}(\ln S);\ \rho U \frac{dU}{dx} + \frac{dP}{dx} = 0;\ \frac{de}{dx} - \frac{P}{\rho^2}\frac{d\rho}{dx} = 0 \quad (3)$$

Equations of balances of mass and energy of the mixture components

$$\rho U \frac{d\eta_j}{dx} = -M_j, j = 1,2,3;\ \frac{de_j}{dx} - \frac{P}{\rho_j^2}\frac{d\rho_j}{dx} = 0, j = 1, 3 \quad (4)$$

Equation which expresses the condition that both reaction products have the same temperature

$$P(1 - \frac{\Gamma_2 c_{v2}}{\Gamma_4 c_{v4}}) = B_2 \rho_2^m - \frac{\Gamma_2 c_{v2}}{\Gamma_4 c_{v4}} B_4 \rho_4^n \quad (5)$$

Additivity rules for energy and density of the mixture and the balance equation for mass fractions of the mixture components

$$e = \sum \eta_i e_i,\ 1/\rho = \sum \eta_i / \rho_i,\ \sum \eta_i = 1 \quad (6)$$

Equations of state for solid

$$P = \Gamma_j \rho_j (e_j - e_{0j}) + B_j [(\frac{\rho_j}{\rho_{j0}})^{l_j} (1 - \frac{\Gamma_j}{l_j - 1}) - \Gamma_j - 1 + \frac{\rho_j}{\rho_{j0}} \frac{\Gamma_j l_j}{l_j - 1}], j = 1, 3 \qquad (7)$$

and that for products

$$P = \Gamma_j \rho_j (e_j - e_{0j}) + B_j \rho_j^{m_j} (1 - \frac{\Gamma j}{m_j - 1}), j = 2, 4 \qquad (8)$$

Here S is the cross-section area of the flow tube; M is the intensity of chemical conversion per unit volume; Γ is the Gruneizen parameter, and c_v is the heat capacity. Index «0» denotes initial conditions. Chemical energy released due to conversion is the difference between values e_{0j} of corresponding components.

The coefficients in (7) are determined from the literature data on Hugoniot and Gruneisen coefficient. The coefficients in (8) are adjusted to get a best approximation of the CJ detonation parameters. These were calculated with the TDS thermodynamic code [Victorov (2002)] using be6 EOS; the initial densities of explosive material having been varied to get the detonation pressure range expected in the studied LVD process.

In order to close the ODE system, the right term of the mass conservation equation of the mixture (3) responsible of the flow divergence effect has to be approximated.

For unconfined charges, a standard procedure (for instance, following [Bdzil and Stewart (1989)], [Swift and Lambourn (1993)]) enables one to relate the divergence term with the local front curvature. The same approach can be used for confined charges if the charge diameter is much greater than the reaction zone thickness, and the detonation velocity exceeds sound speed of the confinement material. However, that is not a case considering here because of two significant reasons. First, the acoustic speed in steel (5400 m/s) is higher than the measured detonation velocities ranged from 1500 up to 3500 m/s. There is no steady-state theoretical solution for detonation wave structure in this case. In work [ ] for modeling this situation the approach based on acoustic properties of confinement material and evaluation of average angle of deflection of streamline at the interface confinement/detonation products of a detonation has been considered. However, this approach does not enable one to take into account experimental observations [Belyaev, et al (1975), Мияке] which show that the process is governed by inertial and strength properties of confinement, in particular, by the wall thickness of confinement, but acoustic ones. Second, it is reasonable to expect that the ratio of the reaction zone thickness to the charge diameter is near unity and can not be correctly considered as a small quantity. Thus, our model simply assumes that the front curvature effect is small and can be ignored, and the flow divergence is defined by radial expansion of the tube. It yields

$$d(\ln S)/dx = 2V_r/(RD) \qquad (9)$$

where R is the local channel radius, and V_r is the radial velocity of the channel expansion that can be calculated by integrating the equation:

$$\rho_W H_c D(R_c + H_c/2) \frac{dV_r}{dx} = \begin{cases} R(P - P_W) \\ 0, \quad P < P_W \end{cases} \qquad (10)$$

where H_c and R_c are the wall thickness and the initial radius of the channel, ρ_W and Y are the density and yield strength of tube material, and $P_W = Y \ln(1 + H_c / R_c)$ is the strength of the tube. Equation (10) is obtained using the assumptions that ideal plasticity controls the tube deformation and that the effects of tube material compressibility and decrease in tube strength P_W during the tube deformation can be ignored.

The ODE system is integrated from the shock front (x=0) up to the singular sonic point where heat release rate is compensated by energy loss due to lateral expansion of the flow. For charges confined in steel tubes, the unique solution which begins at x=0 and passes through this singular point, defines the detonation velocity D as an eigenvalue of the problem. The solution is obtained by numerical “shooting”.

RESULTS OF ANALYSIS

We have examined the model analyzing our experimental data on non-ideal detonation of industrial AN in prills (1 – 2 mm in grain size, gravimetric density ρ_o=690 kg/m^3) confined in thin-walled steel tubes [Ermolaev, et al (2005b) and (2005c)]. The coefficients used in the numerical modelling are: e_{10} = -4.56 MJ/kg, Γ_1 = 0.9, l = 7.2, B_1 = 1.12 GPa (the best fitting to the experimental Hugoniot D =2.2 + 1.96 U which corresponds to AN of TMD [Dobratz (1981)]), e_{20} = -6.16 MJ/kg, Γ_2 = 0.53, m = 3.745, B_2 = 0.95E-02 Pa, Y = 0.22 GPa and η_{2f} = 0.01. Thermodynamic detonation parameters for AN of this density as well as for the AN + Al mixtures are shown in Table 1. Fig. 33 shows numerical simulation results together with experimental data. As is seen, adjusting two parameters of the AN burning law one can get reasonable agreement between numerical simulation and experiment on the confined LVD velocity vs. charge diameter. The best fit of simulation results to the experiment is obtained with the reaction rate coefficient G_1 = 0.034 μs^{-1} and n=1.1. The results calculated with ±15 % variation of G_1 and n are also shown in Fig.33 to demonstrate a possible inaccuracy of these parameters. Let au notice that the modelling covers the 0.5 – 3 GPa pressure range; and at the detonation velocity 1.9 km/s, the reaction zone thickness and the amount of burnt AN equal 21 mm and 0.68, respectively, and the tube expansion at the CJ locus is 16 %.

Table 5. Thermodynamic characteristics of the CJ detonation in AN + Al mixtures 700 kg/m^3 in density

	Neat AN	AN + 2 % Al	AN + 8 % Al	AN + 12 % Al	AN + 18.5 % Al
D, m/s	3382	3505	3630	3640	3580
P, GPa	2.04	2.28	2.63	2.72	2.73
T, K	1773	2117	2970	3490	4240
U, m/s	860	930	1030	1106	1120
Q, MJ/kg	1.47	2.04	3.65	4.72	6.38

Numerical modeling was implemented for AN mixtures with 18.5 % (neutral oxygen balance), 8 % and 2% Al. Input parameters for AN (as a component of the mixture) are the same as in the aforesaid modeling. For Al we used: ρ_{30} = 2700 kg/m^3, e_{30} = -0.415 MJ/kg, Γ_1 = 2.0, l = 6.0 and B_1 = 11.5 GPa (according to the experimental Hugoniot D = 5.35 + 1.34 U). For the AN + Al reaction products we used e_{40} = -10.1 MJ/kg, Γ_4 = 0.22, m = 3.653 and B_4 = 0.01286 Pa; ρ_W = 7800 kg/m^3, Y = 440 MPa, H_c = 2 mm and η_{2f} = 0.01.

At first, we have examined the evident assumption that the burning rate of AN in the AN + Al mixtures is the same as in the case of the neat AN (i.e., G_1 = 0.034 μs^{-1} and n = 1.1). Fig. 35 illustrates the results of this examination for the AN + 2% Al mixture. However, it should be noted that in experiments with AN+ Al mixtures we used the steel tubes of 2 mm wall thickness that is smaller than in runs with the neat AN. Because of strong effect of the tube thickness, we show on Fig. 35 for comparison the modelling data which predicts the detonation velocities of AN prills as if they were tested with the same confinements as the mixtures.

As is seen from simulation results, addition of 2% Al significantly enhances detonability of AN. This effect is in a qualitative agreement with experimental data. However, the calculated detonation velocities turn out to be markedly less than experimental ones even at the maximum rate of the Al burning, which is attained when the decrease of concentration of the AN conversion products in the reactive fluid begins to limit the Al consumption. Hereupon, in order to get agreement with experiment, the higher value of the parameter G_1 = 0.05 μs^{-1} has to be used.

Figs. 36 – 38 show the calculation results for mixtures of AN with 2%, 8% and 18.5% Al of two different particle sizes, together with the corresponding experimental data for comparison. As is seen, numerical modeling enables to reproduce the dependencies of the confined detonation velocity in

mixtures of AN prills with Al (5 μm) on the charge diameter and Al content by using the same set of conversion rate parameters (G_1 = 0.05 μs^{-1}, n = 1.1 and G_{Al} = 0.03 μs^{-1}). The best agreement between modeling and experiment is observed in the case of the AN + 8% Al mixture. In the mixtures with 2% Al and 18.5 % Al, modeling predicts more monotonous dependence on the charge diameter than one observes in experiment. The effect observed when the fine (5 μm) Al is replaced by the coarse (45 μm or 100 μm) Al can be reproduced numerically by significant decrease of the Al burning rate. For the mixture with 2 % Al (coarse) the best consent between modeling and experiment has been obtained by using G_{Al} = 5E-4 μs^{-1}, and for the mixtures with 8 % and 18.5 % of coarse Al by using G_{Al} = 1.5E-3 μs^{-1}. It means that the burning time of Al particles under the considered detonation conditions is roughly proportional to the Al particle diameter with exponent near 1.5.

Finally, Fig. 39 gives an example of the space profiles of the wave parameters calculated for the AN + 8% Al (5μm) mixture, charge diameter 16 mm and detonation velocity 2130 m/s.

CONCLUSIONS

Velocity of non-ideal detonation propagating in the AN prills + Al mixtures in the charges confined in thin-walled steel tubes has been recorded. Effects of the Al content and particle size as well as the effect of the charge diameter varied from 8 to 31 mm have been studied. All steel tubes were 1 m long. The plastic explosive booster which used for detonation initiation produces in the mixture an over-compacted wave. Monitoring the wave propagation along the charge shows that the transformation of the initial wave into a self-sustained steady detonation takes rather long distance, and in a few runs (with the mixtures comprising coarse Al particles) the wave velocity is permanently decreasing along the whole charge length. The detonation velocity is determined as average value over three last measurement bases, and covers depending on parameters varied a range from 1100 up to 4500 m/s. An expected level of the pressure in detonation front is from 0.7 up to 4 GPa.

Experimental data on non-ideal detonation has been numerically analyzed by using the simplified quasi-1D model of a steady low velocity detonation. With the best-fitting values of varied parameters which set the burning rates of AN and Al, numerical modeling reasonably reproduces detonation velocity and its behavior observed in experiment. The corresponding analysis implemented by taking into account experimental data on a nonideal detonation of AN prills has shown that in the mixtures with Al, ammonium nitrate burns essentially faster (approximately in 1.5 times) than in absence of the additive. This conclusion confirms results obtained earlier [ ] by analysis of the detonation velocity vs. charge diameter data published for unconfined AN + Al mixtures in [ ]. The following values of varied parameters provide the best agreement between modeling and experiment for mixtures with Al (5 μm): G_1 = 0.05 μs^{-1}, n = 1.1 and G_{Al} = 0.03 μs^{-1}. To reproduce a decrease in detonation velocity observed if fine Al (5 μm) is replaced by coarse Al (45 μm) or Al (100 μm), the parameter factor G_{Al} should be decreased by 20 – 60 times. It approximately corresponds to dependence of Al burning rate on charge diameter in power 1.5.

REFERENCES

10) Ermolaev B.S., Khasainov B.A., Presles H.-N., and Vidal P. (2005) A Simple Approach for Modelling Reaction Rates in Shocked Multi-Component Solid Explosives // Proceed. European Combustion Meeting (ECM2005), Lourain-la-Neuve, Belgium, April 3-6, 2005.

11) Ermolaev B.S., Khasainov B.A., Presles H.-N., Vidal P., and Sulimov A.A. (2005) Low velocity detonation in ammonium nitrate and its mixtures. // X111 Russian Symp. on combustion and explosion, Chernogolovka, Moscow region, 7–11 Febr. 2005, report No 155.

12) Nigmatulin, R. I. (1987) Dynamics of Multi-phase Media. // Nauka Press, Moscow (in Russian).

13) Victorov S.B. (2002) The Effect of Al2O3 Phase Transitions on Detonation Properties of Aluminized Explosives // 12th Int. Det. Symp., August 11 - 16th, San Diego, Ca.

14) Khasainov B.A., Attetkov A.V., and Borisov A.A. (1996) Shock-wave Initiation of Porous Energetic Materials and Visco-Plastic Model of Hot Spots // Chem. Phys. Reports, V. 15 (7), P. 987.

15) Apin A.Ya. (1950) // Doklady Akademii Nauk SSSR, V.50, P.285 (in Russian).

16) Stewart D.S., and Yao J. The normal Detonation Shock Velocity – Curvature Relationship for Materials with Nonideal Equation of State and Multiple Turning Points // Combustion and Flame, 1998, v.113, No 1-2, p.224-235.

17) Khasainov, EFAE

18) Brun, L., Kneib, J.-M., and Lascaux, P. (1993) Computing the Transient Self-Sustained Detonation after a New Model //10th Int. Det. Symp., Boston, Ma., July 12-16, ONR 33395-12, P. 43.

19) Leuret F., Chaisse F., Presles H.N., and Veyssiere B. (1998) Experimental Studies of the Low Velocity Detonation Regime during the Deflagration to Detonation Transition in a High Density Explosive // 11th Int. Det. Symp., August 31–Sept. 4, Snowmass, Co, ONR 333000-5, P. 693.

Apin A.Ya. (1945) Influence of Physical Structure and Aggregate State on Detonability of High Explosives // Dokladi Akademii Nauk SSSR, V. 50, p. 285-289.

Bdzil J. and Stewart D.S. (1989) Modeling Two-Dimensional Detonations with Detonation Shock Dynamics // Phys. Fluids, 1989, A 1, p. 1261 – 1267.

Belyaev A.F., Bobolev V.K, Korotkov A.I, Sulimov A.A., and Chuico S.V. (1975) Transition from deflagration to detonation in condensed phases // Translated from Russian by Israel program of scientific translation. - Jerusalem. - 1975. (NTIS TT 74-50028).

Borisenok V.A., Simakov V.G., etc. (2003) PVDF-gauge of Dynamic Pressure : Theory and Experiment // Substances, Materials and Constructions under Intensive Dynamic Interactions, editor Michailov A.L., VNIIEF, Sarov, 2003, pp. 437 – 441.

Dobratz B.M. (1981) LLNL Explosives Handbook // LLL, Livermore, Ca, UCRL-52997, 1981.

Dokhan A., Price E.W., Seitzman J.M., and Siegman R.K. (2003) // 39th AIAA/ASME/SAE/ ASEE Joint Propulsion Conference and Exhibition, July 20-23 2003. Huntsville, Al, USA.

Eyring H, Powell RE, Duffrey GH, Darlin RB (1949) The stability of detonation // Chemical Reviews, V. 45, p. 69-181.

Ermolaev B.S., Belyaev A.A., Sulimov A.A. (2004) Numerical Modelling the Deflagration-to-Detonation Transition in Pyroxilin Propellants // Chemical Physics Report, V.23, No 1, p.62-72.

Ermolaev B.S., Belyaev A.A., Sulimov A.A. (2005) Numerical modelling of Convective Burning of Porous Composite Systems Based on Ammonium Perchlorate and Fine Aluminium Powder // Chemical Physics Report, V.24, No 1, pp.84 – 94 (in Russian).

Ermolaev B.S., Khasainov B.A., Presles H.-N., Vidal P. (2005b) A Simple Approach for Modelling Reaction Rates in Shocked Multi-Component Solid Explosives // European Combustion Meeting 2005. Louvain-la-Neuve, Belgium.

Ermolaev B.S., Khasainov B.A., Presles H.-N., Vidal P., Sulimov A.A. (2005c) Low Velocity Detonation in Ammonium Nitrate and Its Mixtures // Proceedings of 13-th All-Russian Symposium on Combustion and Explosion, February 2005, Chernogolovka, Moscow Region, Report No 155.

Ermolaev B.S., Sulimov A.A., Presles H.-N., Khasainov B.A., etc. (2006) Spontaneous Explosion of Ammonium Nitrate in a Contact with a Compound which, Being Dissolved in Water, Releases Active Chlorine // Paper submitted for publication into "Chemical Physics Report".

Glazkova A.P. (1976) Catalysis of Burning of Explosives // "Nauka" Publisher, M. (in Russian).

Khasainov B.A., Ermolaev B.S., Presles H.-N. (1993) Effect of Glass Microballoons on Shock Wave Sensitivity and Detonation Critical Diameter of Condensed Explosives // Tenth International Symposium on Detonation, Office of Naval Research, ONR 33395-12, P. 749-757.

Khasainov B.A., Attetkov A.V., and Borisov A.A. (1996) Shock-wave Initiation of Porous Energetic Materials and Visco-Plastic Model of Hot Spots // Chem. Phys. Reports, 1996, V. 15 (7), p. 987-1062.

Khasainov B.A., Ermolaev B.S., Presles H.-N., Vidal P. (1997) On the effect of grain size on shock sensitivity of heterogeneous high explosives // Shock Waves, V. 7, 1997, P. 89-105.

Khasainov B.A., Ermolaev B.S., Presles H.-N., Vidal P. (2002) Numerical Modeling of Nonideal Detonations in Ammonium Nitrate/Aluminium Mixtures and Their Blast Effect // 12th International Detonation Symposium, August 11 - 16th, 2002, San Diego, Ca.

Leiper G.A., Cooper J. (1993) Reaction of aluminium and ammonium nitrate in nonideal heterogeneous explosives // Tenth International Detonation Symposium, ONR 33395-12, p.267-275.

Mader Ch. L. (1979) Numerical modeling of detonations // University of California Press, Berkeley- Los Angeles – London.

Molodets A.M., Eremchenko E.N. (1994) Summarized Dependence of Electrical Response of Polymer Piezo-film on the Shock Compression Pressure // Fizika goreniya i vzryva, V.30, No 2, 1994, p. 149 – 154.

Nabatov S.S., Yakushev V.V. (1994) Analysis of the Response of Piezo-Polymer Pressure Gauges on a Plane Shock Wave // Fizika goreniya i vzryva, V.30, No 2, 1994, p. 130 – 135.

Nigmatulin R. I. (1987) Dynamics of Multi-phase Media. Nauka Press, Moscow (in Russian).

Pochil P.F., Belyaev A.F., etc. (1972) Combustion of Powdered Metals in Active Media // "Nauka" Publisher, Moscow. (in Russian).

Rozdestvenskii B.L., Yanenko N.I. (1968) Systems of Quasi-Linear Equations and Their Application in Gas Dynamics // "Nauka" Publisher, M. (in Russian).

Soulard L., Bauer F. (1990) Applications of Standardized PVDF Shock Gauges for Shock Pressure Measurements in Explosives // Shock compression of condensed matter –1989, Editors Schmidt S. C. et al. Elsevier, Amsterdam, 1990, P. 817-820.

Swift D.C, and Lambourn B.D. (1993) A Review of Developments in the W-B-L Detonation Model // 10th Int. Detonation Symposium, July 12-16, 1993, p. 386-393, ONR 33395-12.

Victorov S.B. (2002) The effect of Al_2O_3 phase transitions on detonation properties of aluminised explosives. // Twelfth International Symposium on Detonation. San Diego, 2002.

FIGURES

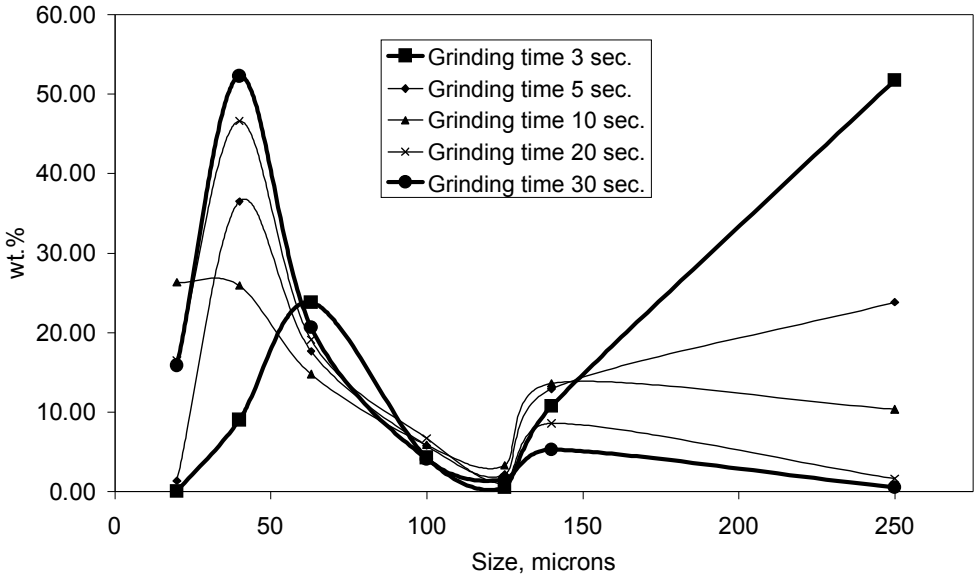

Figure 1. Distribution of AN particles by sizes for different times of grinding for the samples with the same mass.

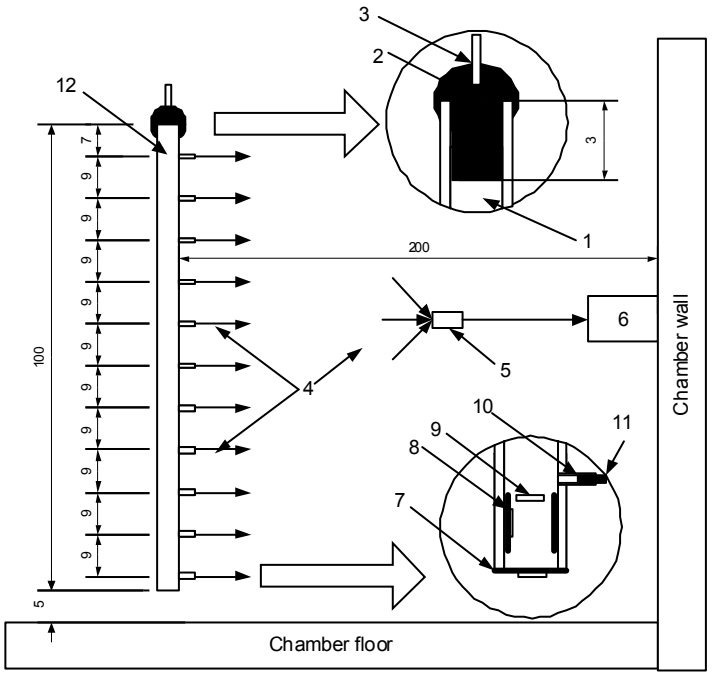

Figure 2. Schematic of the setup together with sizes (in cm) and location of gauges and probes:
(1) mixture tested, (2) booster, (3) detonator-cap, (4) optical fibers, (5) collector of light emission, (6) photodiode together with preamplifier, (7) 200 μm Al foil, (8) a holder for PVDF gauges, (9) positions of PVDF sensors, (10) steel capillary tube, 11 – optical fibre, (12) steel confinement in assembly.

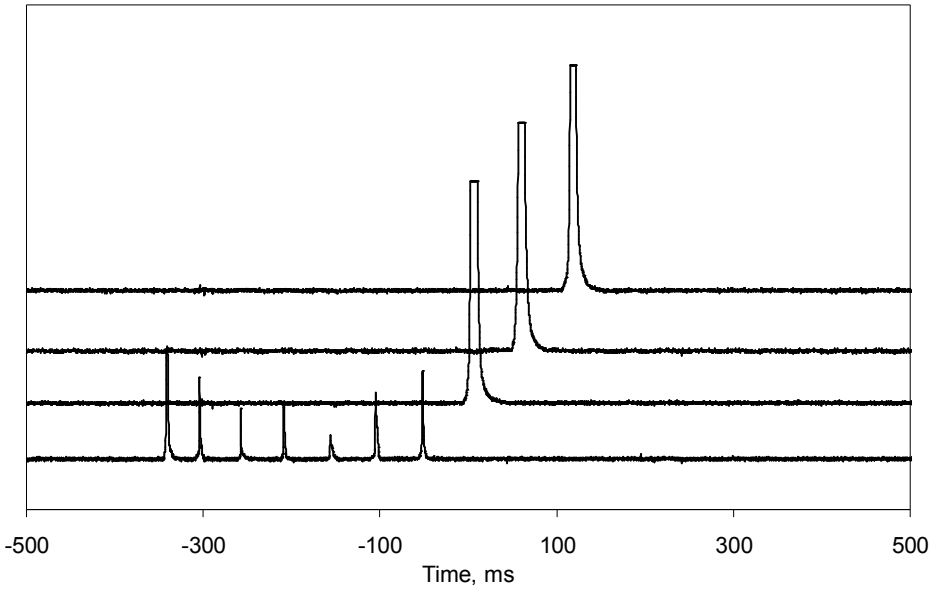

Figure 3. An example of optic fiber signals recorded in exp.1. The case when seven probes are collected together and each signal of three other probes are recorded separately.

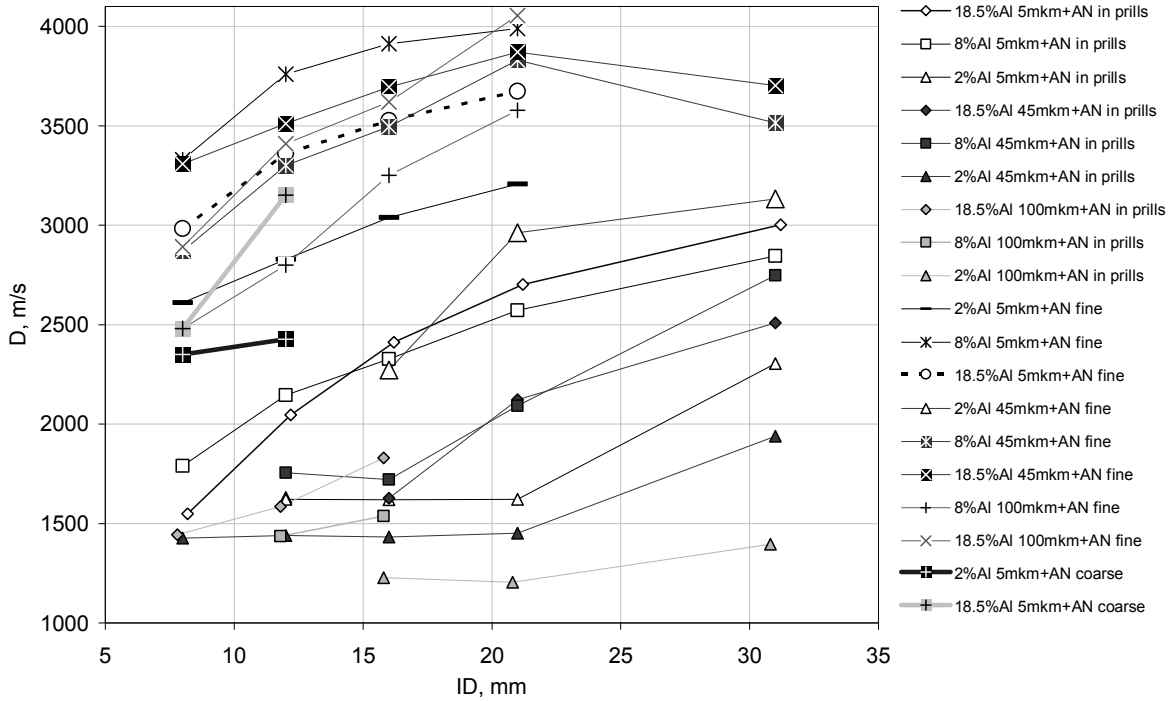

Figure 4. Overall results as detonation velocity versus charge diameter are presented here. All diagrams excluding points for pure AN are presented for tubes with same wall thickness (2 mm). Diagrams shows in same time a great effect of particles sizes, tube diameters and mixture richness.

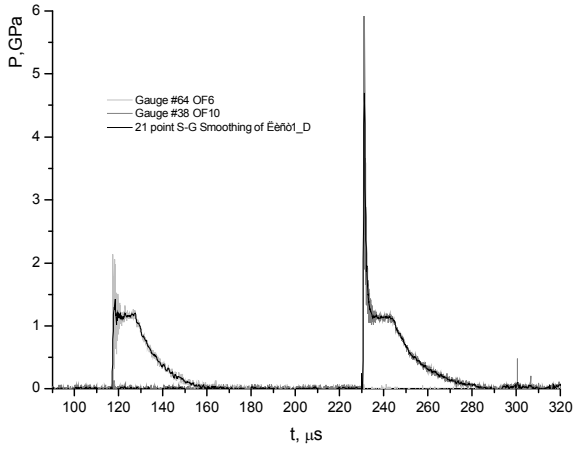

1)

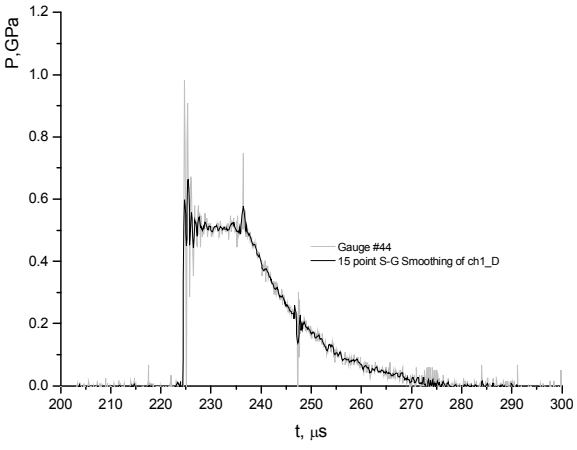

2)

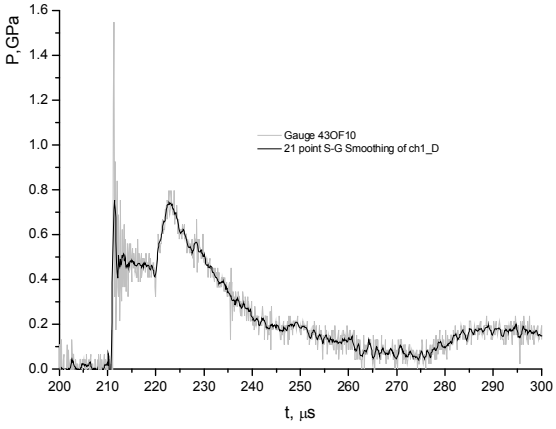

3)

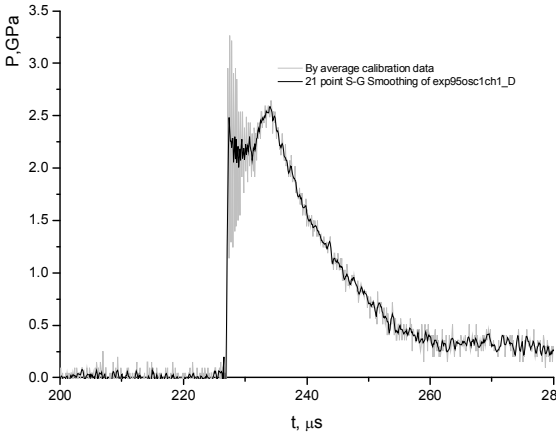

4)

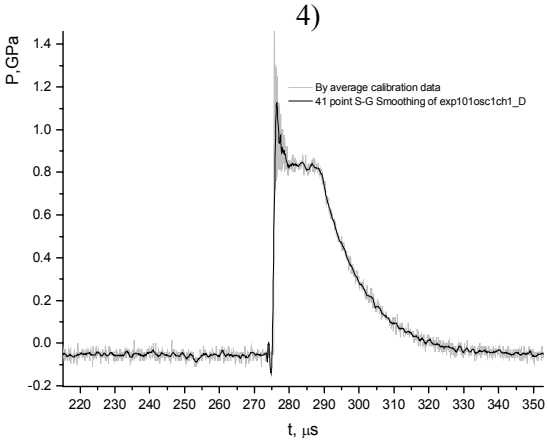

5)

Figure 5. Pressure traces selected from experiments with grinded AN.

1) Mixture: 2 wt.% Al 5 μm + AN 30s in ∅21. Two gauges mounted in front of 6th and 10th optical fibers (390 and 890 mm from the beginning of the tube respectively)
2) Mixture: 8 wt.% Al 5μm + AN 30s in ∅12. One gauge mounted in front of 10th optical fiber
3) Mixture: 8 wt.% Al 5 μm +AN 30s in ∅16. One gauge mounted in front of 10th optical fiber
4) Mixture: 18.5 wt.% Al 45 μm + AN30s in ∅16. One gauge mounted in front of 10th optical fiber
5) Mixture: 2 wt.% Al 45 μm + AN30s in ∅21. One gauge mounted in front of 10th optical fiber

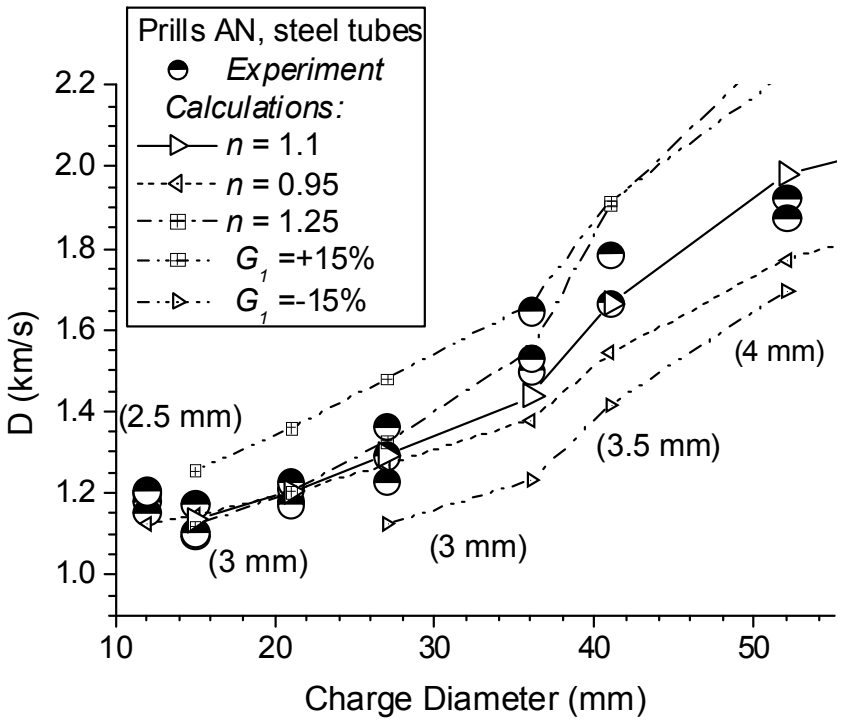

Figure 33. Low velocity detonation in IAN prills confined in steel tubes of different charge diameter and wall thickness (values in round brackets). Comparison between numerical simulations and experiment, and illustration of sensitivity of detonation velocity to the 15% change of the reaction rate coefficients. The best fitting set corresponds to $G_1 = 0.034\ \mu s^{-1}$ and n = 1.1.

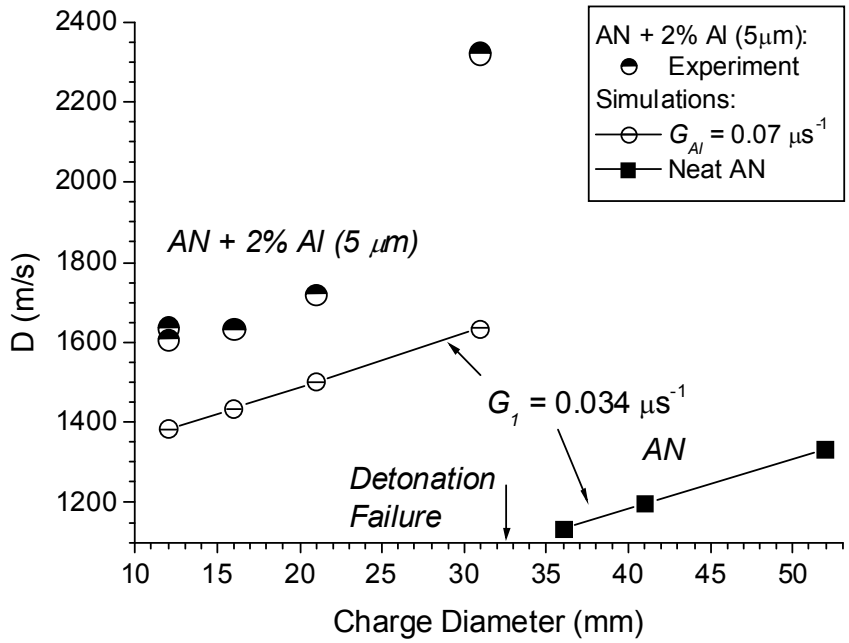

Figure 35. The simulation results demonstrating that AN in the AN + 2% Al mixture burns quicker than with no Al additive

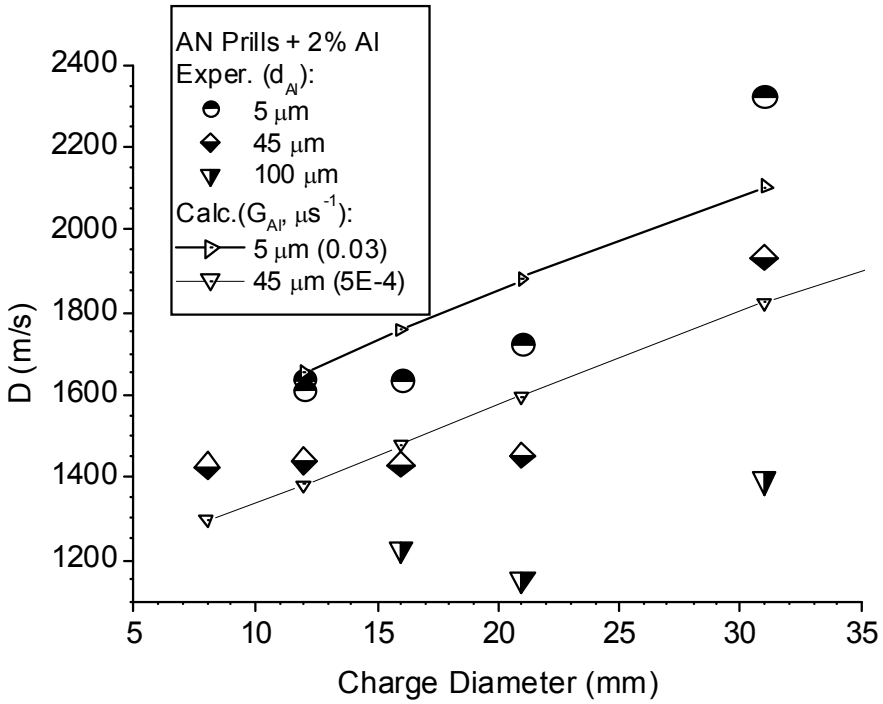

Figure 36. Dependence of the confined detonation velocity in the AN + 2% Al mixtures on the charge diameter and Al particle size. Comparison between modelling and experiment.

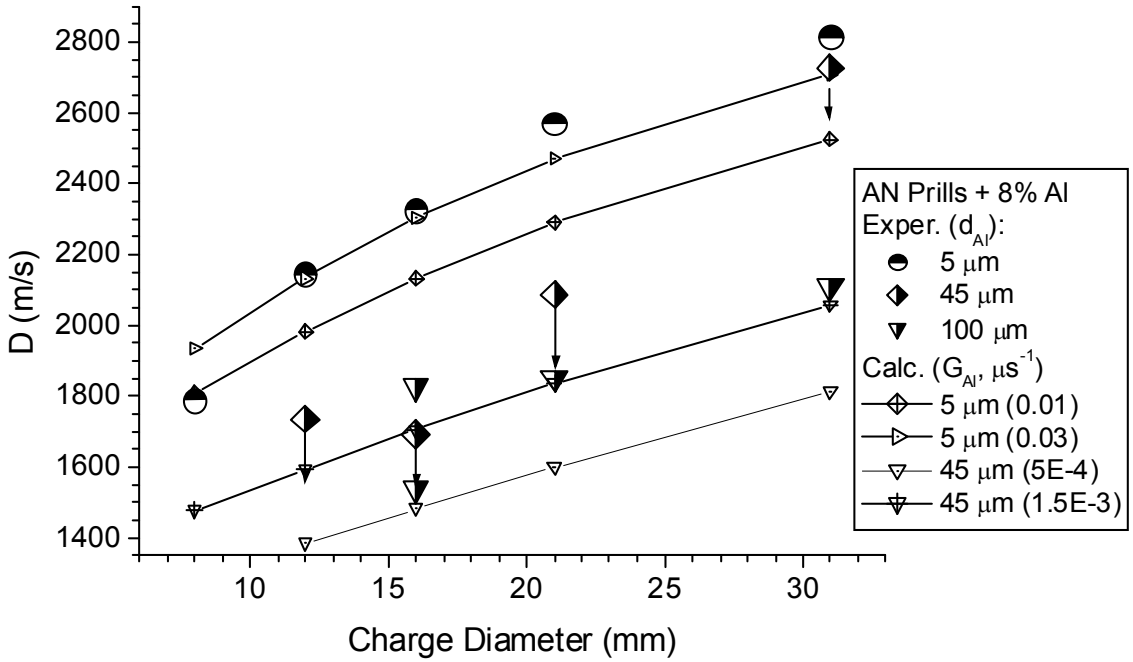

Figure 37. Dependence of the confined detonation velocity in the AN + 8% Al mixtures on the charge diameter and Al particle size. Comparison between modelling and experiment.

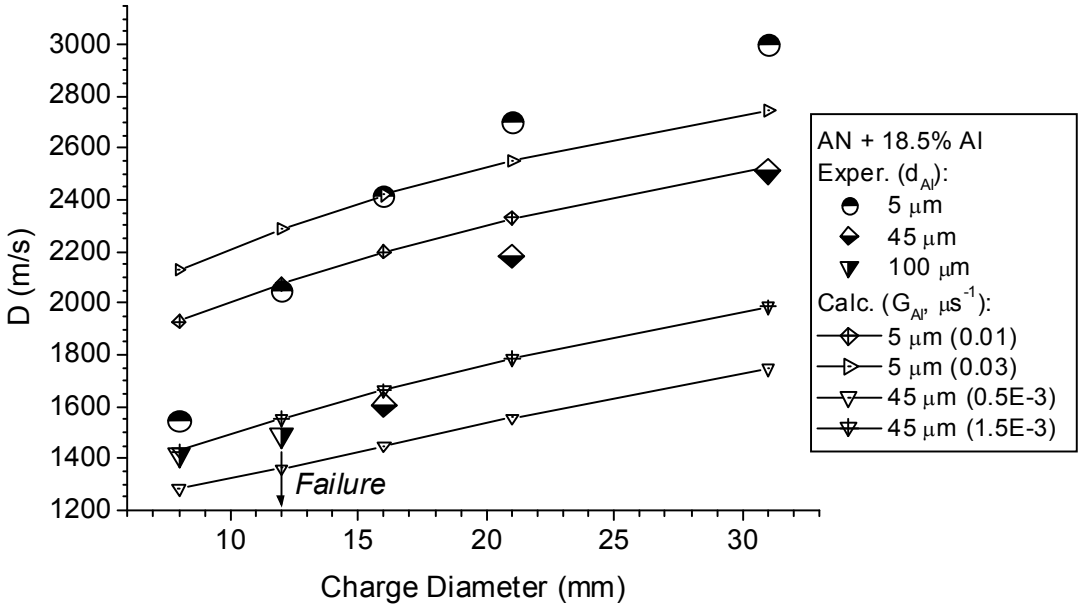

Figure 38. Dependence of the confined detonation velocity in the AN + 18.5% Al mixtures on the charge diameter and Al particle size. Comparison between modelling and experiment.

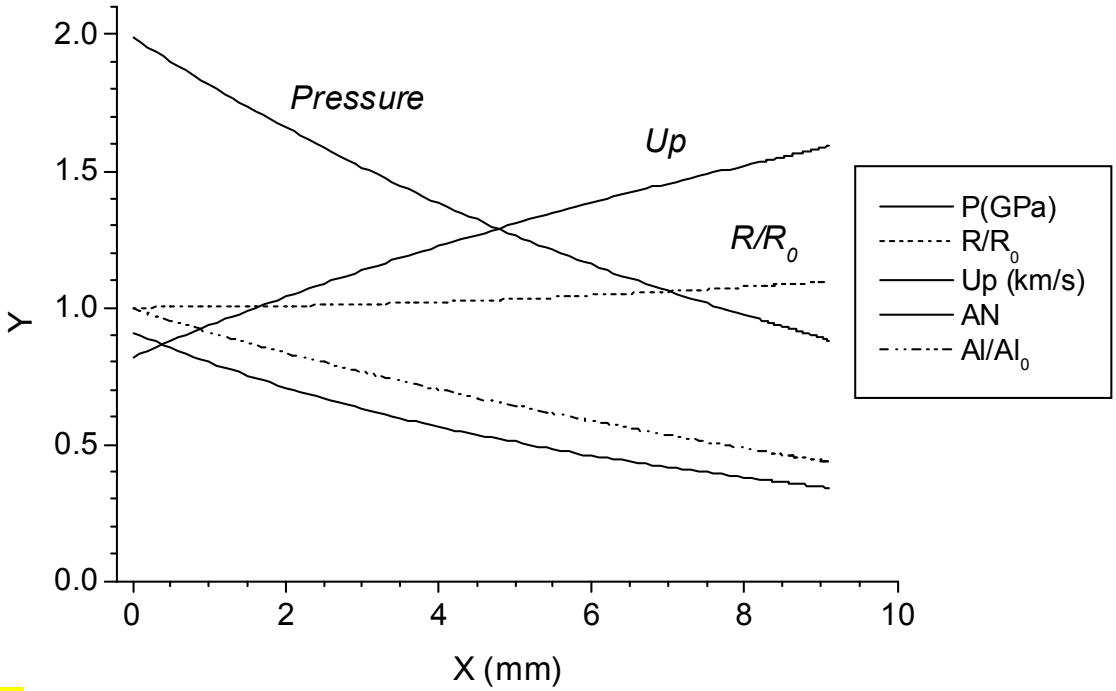

Figure 39. An example of profiles of the pressure, charge radius, particle velocity, and concentrations of AN and Al unburnt for the AN + 8% Al (5μm) mixture, charge diameter 16 mm and detonation velocity 2130 m/s.